Research article

Liying Zhang, Xiangqian Xiu*, Yuewen Li, Yuxia Zhu, Xuemei Hua, Zili Xie, Tao Tao, Bin Liu, Peng Chen, Rong Zhang* and Youdou Zheng

Solar-blind ultraviolet photodetector based on vertically aligned single-crystalline β-Ga_2O_3 nanowire arrays

https://doi.org/10.1515/nanoph-2020-0295
Received May 19, 2020; accepted August 25, 2020; published online September 11, 2020

Abstract: Vertically aligned nanowire arrays, with high surface-to-volume ratio and efficient light-trapping absorption, have attracted much attention for photoelectric devices. In this paper, vertical β-Ga_2O_3 nanowire arrays with an average diameter/height of 110/450 nm have been fabricated by the inductively coupled plasma etching technique. Then a metal-semiconductor-metal structured solar-blind photodetector (PD) has been fabricated by depositing interdigital Ti/Au electrodes on the nanowire arrays. The fabricated β-Ga_2O_3 nanowire PD exhibits ~10 times higher photocurrent and responsivity than the corresponding film PD. Moreover, it also possesses a high photocurrent to dark current ratio (I_{light}/I_{dark}) of ~10^4 and a ultraviolet/visible rejection ratio ($R_{260\,nm}/R_{400\,nm}$) of 3.5×10^3 along with millisecond-level photoresponse times.

Keywords: inductively coupled plasma etching; solar-blind photodetector; vertical β-Ga_2O_3 nanowire arrays.

1 Introduction

Solar-blind region refers to the ultraviolet (UV) radiation with wavelengths of 200–280 nm from the sun, which is strongly absorbed by ozone in the atmosphere and almost nonexistent at the Earth's surface. Photodetectors (PDs) operating in this region without interference from solar radiation have a significant application value in civil and military areas [1–4]. Recently, Ga_2O_3 has gained added interest as a promising candidate for solar-blind photodetection because of its wide bandgap of 4.5–4.9 eV, good chemical and thermal stability [5–8]. Ga_2O_3-based solar-blind PDs are mainly fabricated on β-Ga_2O_3 with different forms, including single crystals [9, 10], thin films [11, 12], individual nanowire/nanowires [13, 14] and nanowire arrays [15–17]. Among them, vertical nanowire arrays can exhibit obvious advantages in optical absorption and carrier generation due to high surface-to-volume ratio and effective light-trapping absorption, which will enable Ga_2O_3 PDs with higher performance. At present, Ga_2O_3 nanowire arrays are mostly obtained by the bottom-up epitaxy method [15, 17, 18]. Wang et al. [17] have prepared β-Ga_2O_3 nanowire arrays using hydrothermal and post-annealing method, and the fabricated nanowire PD has a responsivity of 10.80×10^{-3} A/W and a photoresponse time of 0.38 s. Chen et al. [15] have grown β-Ga_2O_3 nanowire arrays by a simple partial thermal oxidation process and fabricated the Schottky UV PD with a response time in the order of microseconds. Latterly, Li et al. [18] have reported the self-catalyzed metal organic chemical vapor deposition (MOCVD) growth of vertical Ga_2O_3 nanowire arrays. Besides, He et al. [16] have investigated the realization of vertical β-Ga_2O_3 nanowire arrays by thermally oxidizing GaN nanowires grown by molecular beam epitaxy (MBE) and fabricated the PD based on graphene/Ga_2O_3 nanowire arrays heterojunction with the response time in the order of milliseconds. However, the top-down etching approach for β-Ga_2O_3 nanowire arrays is little reported. It is well known that the inductively coupled plasma (ICP) etching is a simple and feasible top-down way to obtain orderly aligned nanostructures, which is widely used for semiconductor patterning. So far, there are only a few reports on the etching properties of β-Ga_2O_3 [19–21].

***Corresponding authors: Xiangqian Xiu and Rong Zhang**, Key Laboratory of Advanced Photonic and Electronic Materials, School of Electronic Science and Engineering, Nanjing University, Nanjing 210023, P. R. China, E-mail: xqxiu@nju.edu.cn (X. Xiu), rzhang@nju.edu.cn (R. Zhang). https://orcid.org/0000-0002-6801-2986 (X. Xiu)
Liying Zhang, Yuewen Li, Yuxia Zhu, Xuemei Hua, Zili Xie, Tao Tao, Bin Liu, Peng Chen and Youdou Zheng, Key Laboratory of Advanced Photonic and Electronic Materials, School of Electronic Science and Engineering, Nanjing University, Nanjing 210023, P. R. China

In this work, the vertically aligned single-crystalline β-Ga_2O_3 nanowire arrays have been realized by the ICP etching technique, and the metal-semiconductor-metal (MSM) solar-blind PD has been constructed with interdigital Ti/Au electrodes on β-Ga_2O_3 nanowires. The photoelectric properties of the fabricated β-Ga_2O_3 MSM PD based on vertical nanowire arrays structure have been studied and compared with the corresponding β-Ga_2O_3 film PD.

2 Experiments

The 1.25 μm β-Ga_2O_3 epitaxial film was grown on (0001) sapphire by halide vapor phase epitaxy (HVPE) at 950 °C for 30 min [22]. High purity O_2 gas and gallium chloride (GaCl) were used as oxygen and gallium source, respectively. The experimental procedure for the fabrication of β-Ga_2O_3 nanowire arrays and the corresponding MSM PD is depicted in Figure 1. First, a 10 nm nickel (Ni) layer was deposited on the β-Ga_2O_3 film by e-beam evaporation and then thermally annealed in N_2 ambient at 850 °C for 3 min to form the isolated Ni nanoparticles as the etching mask. The etching process was conducted under a gas mixture of BCl_3/Ar with the RF/ICP power of 150/700 for 10 min. After the ICP etching, a set of interdigital Ti/Au (20/80 nm) electrodes were made on β-Ga_2O_3 nanowires to construct the solar-blind ultraviolet PD. The electrodes were 3.9 mm long and 3 mm wide with a finger spacing gap of 100 μm. For comparison, a traditional film-type PD with the same electrodes was also fabricated on original HVPE-Ga_2O_3 film.

The morphology and properties of the β-Ga_2O_3 nanowire arrays were characterized by scanning electron microscope (SEM; Gemini 500, Carl Zeiss, Germany), high-resolution X-ray diffraction (XRD; Bruker D8 Advance, Bruker, Karlsruhe, Germany), UV–visible spectrophotometer (UV-6100S) and Ocean Optics UV–VIS spectrophotometer (DH-2000-BAL). The current–voltage (I–V) characteristics of PDs were evaluated by a semiconductor device analyzer (Keithley 2636B). The spectral-responsivity measurements were performed with a photoelectric measurement system consisting of monochromator, Xe lamp source, phase-locked amplifier, and low-noise current preamplifier. The transient response characteristics were measured using a 266 nm pulsed laser and a digital oscilloscope (Tektronix TBS 1102).

3 Results and discussion

Figure 2A and B show the tilted-view and cross-sectional SEM images of high-density β-Ga_2O_3 nanowire arrays after the ICP etching with Ni nanomask. The β-Ga_2O_3 nanowire arrays are composed of vertical nanowire with a uniform height of 450 nm. The average diameter and density of the nanowires are about 110 nm and $1.6 \times 10^8/cm^2$. It is evident that Ni nanomask is a good mask to prevent the ICP etching on the β-Ga_2O_3. Residual metal Ni grains can be clearly seen on the top of nanowires (Figure 2B), which are confirmed by energy dispersive spectroscope analysis (not shown here). Besides, it can be seen that 0.8 μm thick unetched β-Ga_2O_3 film remains under the nanowires.

Figure 2C depicts the XRD patterns of β-Ga_2O_3 nanowires and original film. In addition to the (0006) diffraction peak of sapphire substrate located at 41.7°, three diffraction peaks are observed at 18.9°, 38.4° and 59.0°, which correspond well to $(\bar{2}01)$, $(\bar{4}02)$ and $(\bar{6}03)$ crystal planes of monoclinic β-Ga_2O_3 (JCPDS No. 41-1103). It implies that the original film is single crystal β-Ga_2O_3 with $\bar{2}01$ plane orientation. After the ICP process, all diffraction peaks in the patterns exhibit no change except for a slight decrease of intensities. Figure 2D shows the absorbance spectra of both samples and the inset is the corresponding $(\alpha h\nu)^2$ versus $h\nu$ curves. The absorption onsets of both samples are located at around 270 nm and the β-Ga_2O_3 nanowires can exhibit significantly higher absorbance and steeper

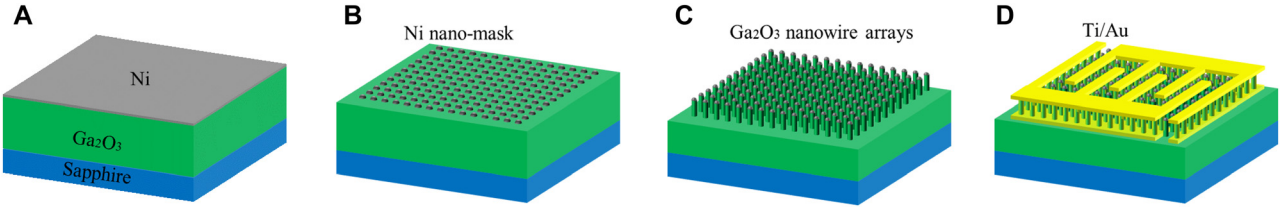

Figure 1: Schematic diagram of the fabrication of β-Ga_2O_3 nanowire arrays and the corresponding metal-semiconductor-metal photodetector (MSM PD).
(A) Depositing Ni thin layer on β-Ga_2O_3/sapphire, (B) preparing Ni nanomask by rapid thermal annealing, (C) inductively coupled plasma (ICP) etching β-Ga_2O_3 nanowire arrays, and (D) depositing the interdigital Ti/Au electrodes.

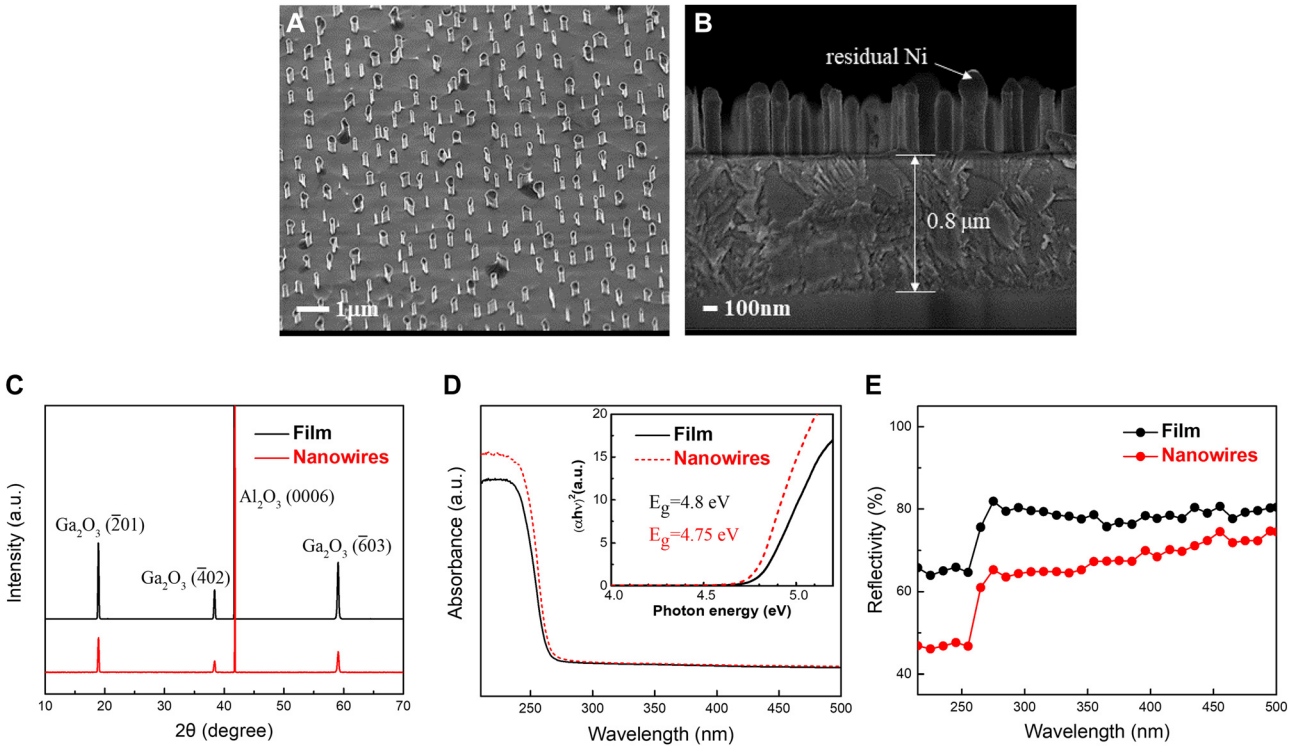

Figure 2: Morphology and characterization of β-Ga_2O_3 nanowire arrays.
(A, B) Tilted-view and cross-sectional scanning electron microscope (SEM) images of vertical β-Ga_2O_3 nanowire arrays. (C–E) X-ray diffraction (XRD) patterns, optical absorbance and reflection spectra of β-Ga_2O_3 nanowires and original film. (Inset) $(\alpha h\nu)^2$ versus $h\nu$.

absorbed edge. In addition, the optical bandgap of the nanowires is evaluated to be ~4.75 eV by the equation: $(\alpha h\nu)^2 = A(E - E_g)$, which is slightly smaller than that of the original film (~4.8 eV). The reflectivity of β-Ga_2O_3 nanowires and original film are shown in Figure 2E. It is obvious that the reflectivity of β-Ga_2O_3 nanowires is lower than that of original film, indicating that the nanowire arrays structure can effectively reduce the surface reflection and thus increase the absorption.

To check the solar-blind photoresponse of the fabricated β-Ga_2O_3 nanowire and film PDs, I–V and spectral response characteristics have been measured. All the I–V curves exhibit linear features in linear coordinates, indicating Ohmic contact of Ti/Au on the β-Ga_2O_3 nanowires and original film. For a better comparison, Figure 3A plots the I–V curves for both PDs in exponential coordinates measured in the dark and under illumination of 254 nm light with an incident power density of 0.5 mW/cm^2. At 5 V applied bias, the dark currents are 2.4×10^{-9} and 4.8×10^{-9} A for β-Ga_2O_3 nanowire and film PDs, respectively. The dark current of β-Ga_2O_3 nanowire PD is slightly smaller than that of β-Ga_2O_3 film PD, which means that the nanowires may have a lower defects and oxygen vacancies density. Under UV illumination (254 nm), the photocurrents of the β-Ga_2O_3 nanowire and film PDs are 2.3×10^{-5} and 2.1×10^{-6} A, respectively. The photocurrent to dark current ratios (I_{light}/I_{dark}) of the β-Ga_2O_3 nanowire and film PDs at the bias of 5 V are ~9.4×10^3 and ~4.6×10^2 A, respectively.

Figure 3B shows the photoresponsivity spectra of the β-Ga_2O_3 nanowire PD measured with different applied biases from 1 to 5 V. It is obvious that the responsivity (R) increases with increasing the bias voltage. The spectral response of the β-Ga_2O_3 film PD measured at an applied bias of 5 V is also plotted for comparison. With an applied bias of 5 V, the peak responsivities measured from the β-Ga_2O_3 nanowire and β-Ga_2O_3 film MSM PDs are 0.122 and 0.01 A/W at λ = 260 nm, respectively. The cutoff ($\sqrt{1/2}\,R_{max}$) occurs at around 270 nm for both β-Ga_2O_3 MSM PDs, which illustrates the good solar-blind nature of the devices. The UV/visible rejection ratio, defined as the ratio of the R at 260 and 400 nm ($R_{260\,nm}/R_{400\,nm}$) are 3.5×10^3 for the nanowire PD and 4.2×10^2 for the film PD, respectively. The inset of Figure 3B shows the peak responsivity of the β-Ga_2O_3 nanowire PD as a function of the bias voltage. The responsivity of the β-Ga_2O_3 nanowire PD

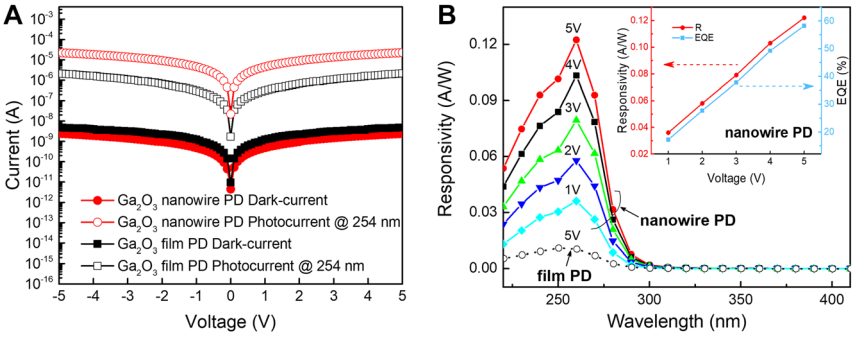

Figure 3: Photoelectric properties of β-Ga_2O_3 nanowire and film photodetectors (PDs).
(A) *I–V* characteristics of PDs measured in dark and under 254 nm light illumination. (B) Spectral responses of PDs measured at different bias voltage.

increases approximately linearly with bias voltage, and the value of external quantum efficiency (EQE), which is calculated by EQE = $hcR_\lambda/(e\lambda)$ [17] is about 58% at the bias of 5 V. In addition, the detectivity (D^*) of the β-Ga_2O_3 nanowire PD is estimated to be 4.4×10^{11} Jones by the expression: $D^* = R_\lambda/\sqrt{2qI_d/S_{\text{effective}}}$. These values are superior to lately reported results for β-Ga_2O_3 MSM PD based on vertical nanorod arrays [17].

The β-Ga_2O_3 nanowire PD has better characteristics than the β-Ga_2O_3 film PD because of the high surface-to-volume ratio of vertical nanowire arrays, which can increase the light absorption and facilitate carrier generation. Figure 4A schematically illustrates the respective light-trapping mechanisms of both PDs. As the UV light illuminates on the nanowire PD, the incident light is scattered between the gaps of the nanowires, which increases the path length of incident light and thus its absorption. In order to verify the enhanced light-trapping effect of the nanowire arrays structure, the finite difference time domain simulations have been adopted to illustrate the light field intensity distribution in β-Ga_2O_3 nanowire and film PDs. As clearly shown in Figure 4B, the light field intensity located in the nanowires is stronger than that in the film. Such a result is in good agreement with the measured absorbance and reflection spectra, indicating that the β-Ga_2O_3 nanowire PD can capture more light energy to generate more carriers, which consequently make higher photocurrent compared to the film PD.

Apart from the light-trapping, the carrier-trapping mechanism mediated by oxygen adsorption and desorption at the β-Ga_2O_3 nanowire surface (Figure 5) is also considered the reason for the enhanced photoresponse [23–25]. In the dark, a large number of oxygen molecules are adsorbed on the nanowire surface and capture free electrons in the nanowire to form negatively charged oxygen ions [O_2 (gas) + e^- ↔ O_2^- (*a*d)], which reduces the carrier

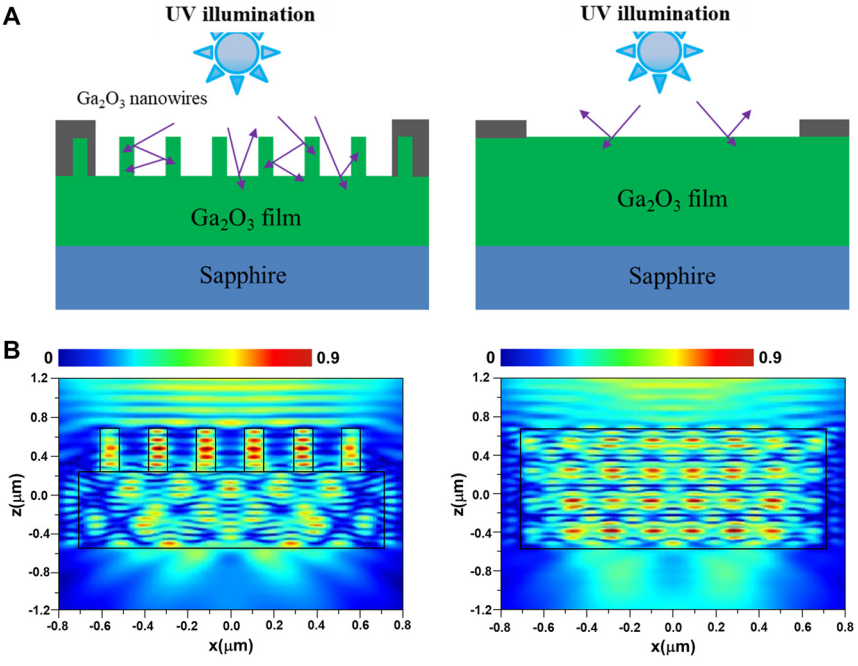

Figure 4: (A) Schematic illustration of the respective light-trapping mechanisms and (B) the simulated light field intensity distribution in β-Ga_2O_3 nanowire and film photodetectors (PDs).

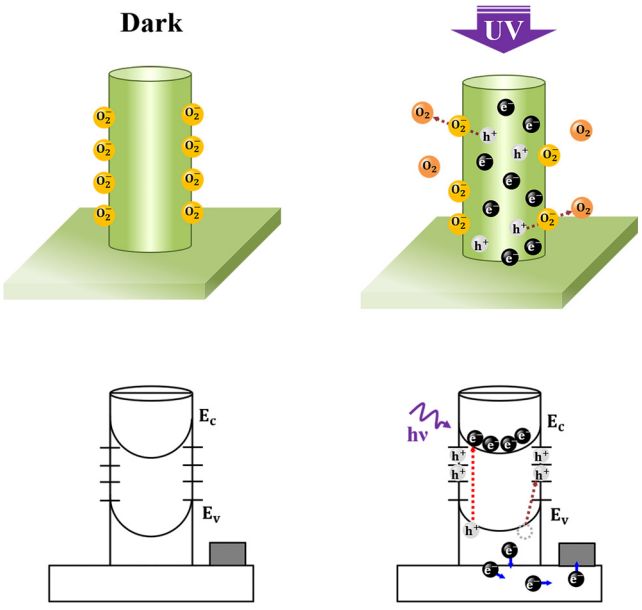

Figure 5: Schematic diagrams of the oxygen molecular sensitization mechanism and energy band of the β-Ga_2O_3 nanowire in the dark and under ultraviolet (UV) illumination.

concentration and creates a low-conductivity depletion layer near the nanowire surface. Under UV illumination, the nanowire absorbs the photons to generate electron-hole pairs. The photogenerated holes migrate to the nanowire surface along the potential slope caused by band bending and oxidize the negatively charged oxygen ions adsorbed on the surface $[O_2^-(ad) + h^+ \leftrightarrow O_2(gas)]$, while the electrons are collected at the core of the nanowires and transferred to the electrode through the film. In this way, the oxygen-related surface trap states at the nanowire surface can reduce photocarrier recombination because of the quick separation, which will give rise to an enhancement in the nanowire photoresponse. The respective schematic energy band diagrams of the β-Ga_2O_3 nanowire in the dark and under UV illumination are also shown in Figure 5.

It should be noted that although the nanowire PD contains both nanowires and film structures, the influence of unetched Ga_2O_3 film on the photoresponse variation is far less than that of nanowires, which is consistent with the simulation results (Figure 4B). Shen et al. [11] have reported the effect of thickness on the performance of solar-blind PD based on β-Ga_2O_3 films. They have obtained the pretty high I_{light}/I_{dark} ratio (6.7×10^4) after thickness optimization (~250 nm). But their results also indicate the change of the thickness on the effect of PD performance is relatively small while the thickness varies from 1.6 to ~1 μm. In our work, the I_{light}/I_{dark} ratio and wavelength responsivity of nanowire PD increase by 10 times in a similar thickness variation range (from 1.25 to 0.8 μm), which means that the nanowire arrays structure should be the major reason for the significantly enhanced photoresponse. Besides, the localized surface plasmon effect of the few residual tiny Ni metal grains on the top of the β-Ga_2O_3 nanowire can also enhance the light absorption of β-Ga_2O_3 nanowires and facilitate photocarrier separation [26, 27].

To quantitatively assess the response rates of the PDs, the time-dependent photocurrents under illumination of

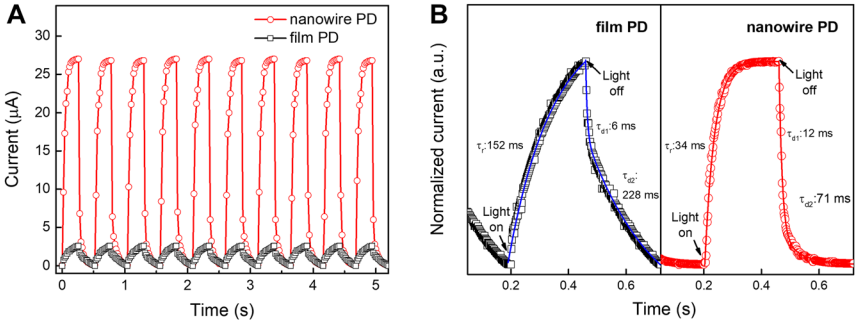

Figure 6: Transient response of photodetectors (PDs) to 266 nm illumination at the bias of 5 V. (A) Responses for multicycles and (B) normalized response for β-Ga_2O_3 nanowire and film PDs.

Table 1: Summary of performance parameters of the β-Ga_2O_3 film and nanowire PDs prepared in this work.

Structure	Bias (V)	I_{dark} (nA)	I_{light} (μA)	R (A/W)	Rejection ratio $R_{260\ nm}/R_{400\ nm}$	Response times (ms)	
						τ_r	τ_{d1}, τ_{d2}
Film	5	4.8	2.1	0.01	4.2×10^2	152	6, 228
Nanowire	5	2.4	22.5	0.122	3.5×10^3	34	12, 71

PDs, photodetectors.

Table 2: Comparison of critical parameters for the state-of-the-art solar-blind PDs based on β-Ga_2O_3 nanowire arrays.

Material and structure	Device	Bias (V)	R (A/W)	EQE (%)	Response times (ms)		I_{light}/I_{dark}	Rejection ratio	Reference
					τ_r	τ_d			
β-Ga_2O_3 nanowires	Schottky	−10	6×10^{-4}	–	10^{-3}	6×10^{-2}	–	2×10^3	[15]
β-Ga_2O_3 nanowires	Schottky	−5	0.185	–	9	8	–	3×10^4	[16]
β-Ga_2O_3 nanorods	MSM	0	1.08×10^{-2}	5.27×10^{-3}	640	380	9.14	–	[17]
β-Ga_2O_3 nanowires	MSM	5	0.122	58	34	12/71	~10^4	3.5×10^3	This work

MSM, metal-semiconductor-metal; EQE, external quantum efficiency; PDs, photodetectors.

a 266-nm pulsed laser with a light density of 1.5 mW/cm^2 have been also investigated. Figure 6A displays the transient responses of β-Ga_2O_3 nanowire and film PDs. It is obvious that both devices exhibit a stable dynamic response in the investigated timescale. Figure 6B shows the response times for the β-Ga_2O_3 nanowire and film PD devices. The photocurrents rise steeply with τ_r of 34 ms for nanowire PD and 152 ms for film PD, respectively. The decaying edges of the currents consist of two different relaxation processes with a fast-response part (τ_{d1}) and a slow-response part (τ_{d2}). For the nanowire PD, the decaying time constants are τ_{d1} = 12 ms and τ_{d1} = 71 ms; while for the film PD, the decaying time constants are τ_{d1} = 6 ms and τ_{d1} = 228 ms. The results of dark/photocurrent, responsivity, UV/visible rejection ratio, and rising/decaying response speed for the two devices are summarized in Table 1. From Table 1, the β-Ga_2O_3 nanowire PD exhibits better photoresponse performance than the β-Ga_2O_3 film PD.

For a comprehensive understanding, a comparison of state-of-the-art β-Ga_2O_3 nanowire array-based PDs with critical parameters is shown in Table 2. It can be seen that our device can achieve comparable or even superior photoresponse to some other previously reported β-Ga_2O_3 nanowire PDs. In spite of this, the quality of the original β-Ga_2O_3 film still needs to be further optimized to reduce the dark current and improve the response time. It should be noted that the nanowire arrays parameters, such as the density and dimension, are not optimized. A larger responsivity and faster response times should be obtained by optimizing the fabrication parameters of the nanowire arrays.

4 Conclusion

In conclusion, a solar-blind PD based on vertically aligned single-crystalline β-Ga_2O_3 nanowire arrays has been demonstrated with good response. Vertically aligned β-Ga_2O_3 nanowire arrays have been fabricated by ICP etching using self-aggregated Ni nanomask as the mask on HVPE-grown β-Ga_2O_3 film. In this work, compared with β-Ga_2O_3 film PD, the fabricated nanowire PD can achieve better characteristics including higher photocurrent and higher responsivity. This phenomenon can be attributed to the high surface-to-volume ratio of nanowire arrays, which would increase light-trapping absorption and facilitate oxygen adsorption and desorption at the β-Ga_2O_3 nanowire surface. Under 260 nm illumination, the β-Ga_2O_3 nanowire PD exhibits a responsivity of 0.122 A/W and UV/visible rejection ratio ($R_{260\ nm}/R_{400\ nm}$) of 3.5×10^3 at 5 V. Furthermore, the improved rising time (τ_r) and decaying time (τ_{d1}/τ_{d2}) are 34 and 12/71 ms, respectively. These results indicate that ICP etching is a simple and feasible method to realize vertically aligned single-crystalline β-Ga_2O_3 nanowire arrays, and the devices based on nanowire arrays may be potentially used in the solar-blind UV photodetection, UV-imaging and high-frequency communication, etc.

Acknowledgments: This work is financially supported by the National Key R&D Program of China (grant no. 2017YFB0404201), the State Key R&D Program of Jiangsu Province (grant no. BE2019103), the Six-Talent Peaks Project of Jiangsu Province (grant no. XCL-107), the Fund from the Solid-state Lighting and Energy-saving Electronics Collaborative Innovation Center, PAPD, and the Fund from the State Grid Shandong Electric Power Company.

Author contribution: All the authors have accepted responsibility for the entire content of this submitted manuscript and approved submission.

Research funding: This work is financially supported by the National Key R&D Program of China (grant no. 2017YFB0404201), the State Key R&D Program of Jiangsu Province (grant no. BE2019103), the Six-Talent Peaks Project of Jiangsu Province (grant no. XCL-107), the Fund from the Solid-state Lighting and Energy-saving Electronics Collaborative Innovation Center, PAPD, and the Fund from the State Grid Shandong Electric Power Company.

Conflict of interest statement: The authors declare no conflicts of interest regarding this article.

References

[1] H. Y. Chen, P. P. Yu, Z. Z. Zhang, et al., "Ultrasensitive self-powered solar-blind deep-ultraviolet photodetector based on all-solid-state polyaniline MgZnO bilayer," *Small*, vol. 12, pp. 5809–5816, 2016.

[2] H. Y. Chen, K. W. Liu, L. F. Hu, A. A. Al-Ghamdj, and X. S. Fang, "New concept ultraviolet photodetectors," *Mater. Today*, vol. 18, pp. 493–502, 2015.

[3] D. P. Chaudhari, M. Ombaba, J. Y. Oh, et al., "Solar blind photodetectors enabled by nanotextured β-Ga_2O_3 films grown via oxidation of GaAs substrates," *IEEE Photonics J.*, vol. 9, p. 2300207, 2017.

[4] Z. Li, Y. Xu, J. Q. Zhang, et al., "Flexible solar blind Ga_2O_3 ultraviolet photodetectors with high responsivity and photo-to-dark current ratio," *IEEE Photonics J.*, vol. 11, p. 6803709, 2019.

[5] H. H. Tippins, "Optical absorption and photoconductivity in the band edge of β-Ga_2O_3," *Phys. Rev.*, vol. 140, pp. 316–319, 1965.

[6] N. Ueda, H. Hosono, R. Waseda, and H. Kawazoe, "Synthesis and control of conductivity of ultraviolet transmitting β-Ga_2O_3 single crystals," *Appl. Phys. Lett.*, vol. 70, pp. 3561–3563, 1997.

[7] Z. Hajnal, J. Miró, G. Kiss, et al., "Role of oxygen vacancy defect states in the n-type conduction of β-Ga_2O_3," *J. Appl. Phys.*, vol. 86, pp. 3792–3796, 1999.

[8] S. J. Pearton, J. C. Yang, P. H. Cary, et al., "A review of Ga_2O_3 materials, processing, and devices," *Appl. Phys. Rev.*, vol. 5, p. 011301, 2017.

[9] T. Oshima, T. Okuno, N. Arai, N. Suzuki, S. Ohira, and S. Fujita, "Vertical solar-blind deep-ultraviolet Schottky photodetectors based on β-Ga_2O_3 substrates," *Appl. Phys. Express*, vol. 1, p. 011202, 2008.

[10] X. Chen, W. Mu, Y. Xu, et al., "Highly narrow-band polarization-sensitive solar-blind photodetectors based on β-Ga_2O_3 single crystals," *ACS Appl. Mater. Interfaces*, vol. 11, pp. 7131–7137, 2019.

[11] H. Shen, K. Baskaran, Y. Yin, et al., "Effect of thickness on the performance of solar blind photodetectors fabricated using PLD grown β-Ga_2O_3 thin films," *J. Alloys Compd.*, vol. 822, p. 153419, 2019.

[12] L. Huang, Q. Feng, G. Q. Han, et al., "Comparison study of β-Ga_2O_3 photodetectors grown on sapphire at different oxygen pressures," *IEEE Photonics J.*, vol. 9, p. 6803708, 2017.

[13] P. Feng, J. Y. Zhang, Q. H. Li, and T. H. Wang, "Individual β-Ga_2O_3 nanowires as solar-blind photodetectors," *Appl. Phys. Lett.*, vol. 88, p. 153107, 2006.

[14] S. Wang, H. Sun, Z. Wang, et al., "In situ synthesis of β-Ga_2O_3 nanowires on flexible substrate and solar-blind photodetector," *J. Alloys Compd.*, vol. 787, pp. 133–139, 2019.

[15] X. Chen, K. W. Liu, Z. Z. Zhang, et al., "Self-powered solar-blind photodetector with fast response based on Au/β-Ga_2O_3 nanowires array film Schottky junction," *ACS Appl. Mater. Interfaces*, vol. 8, pp. 4185–4191, 2016.

[16] T. He, Y. K. Zhao, X. D. Zhang, et al., "Solar-blind ultraviolet photodetector based on graphene/vertical Ga_2O_3 nanowire arrays heterojunction," *Nanophotonics*, vol. 7, pp. 1557–1562, 2018.

[17] S. L. Wang, K. Chen, H. L. Zhao, et al., "β-Ga_2O_3 nanorod arrays with high light-to-electron conversion for solar-blind deep ultraviolet photodetection," *RCS Adv*, vol. 9, pp. 6064–6069, 2019.

[18] J. S. Li, X. D. Zhang, X. Cao, et al., "Self-catalyzed metal organic chemical vapor deposition growth of vertical β-Ga_2O_3 nanowire arrays," *Nanotechnology*, vol. 31, p. 02LT01, 2019.

[19] J. E. Hogan, S. W. Kaun, E. Ahmadi, Y. Oshima, and J. S. Speck, "Chlorine-based dry etching of β-Ga_2O_3," *Semicond. Sci. Technol.*, vol. 31, p. 065006, 2016.

[20] L. H. Zhang, A. Verma, H. L. Xing, and D. Jena, "Inductively-coupled-plasma reactive ion etching of single-crystal β-Ga_2O_3," *Jpn. J. Appl. Phys.*, vol. 56, p. 030304, 2017.

[21] A. P. Shah and A. Bhattacharya, "Inductively coupled plasma reactive-ion etching of β-Ga_2O_3: comprehensive investigation of plasma chemistry and temperature," *J. Vac. Sci. Technol. A*, vol. 35, p. 041301, 2017.

[22] Z. N. Xiong, X. Q. Xiu, Y. W. Li, et al., "Growth of β-Ga_2O_3 films on sapphire by hydride vapor phase epitaxy," *Chin. Phys. Lett.*, vol. 35, p. 058101, 2018.

[23] C. Soci, A. Zhang, B. Xiang, et al., "ZnO nanowire UV photodetectors with high internal gain," *Nano Lett.*, vol. 7, pp. 1003–1009, 2007.

[24] T. Y. Tsai, S. J. Chang, W. Y. Weng, et al., "A visible-blind TiO_2 nanowire photodetector," *J. Electrochem. Soc.*, vol. 159, pp. J132–J135, 2012.

[25] C. H. Lin, R. S. Chen, T. T. Chen, et al., "High photocurrent gain in SnO_2 nanowires," *Appl. Phys. Lett.*, vol. 93, p. 112115, 2008.

[26] Z. Wei, X. Jin, Y. Wei, et al., "High-performance AlGaN metal-semiconductor-metal solar-blind ultraviolet photodetectors by localized surface plasmon enhancement," *Appl. Phys. Lett.*, vol. 106, p. 021112, 2015.

[27] R. F. Tang, G. Q. Li, C. Li, et al., "Localized surface plasmon enhanced Ga_2O_3 solar blind photodetectors," *Optics Express*, vol. 28, pp. 5731–5740, 2020.